available at www.sciencedirect.com

ScienceDirect

journal homepage: www.elsevier.com/locate/biochempharm

Small-molecule inhibition of Aurora kinases triggers spindle checkpoint-independent apoptosis in cancer cells

Lei Sun [a], Dengwen Li [a], Xin Dong [a], Haiyang Yu [a], Jin-Tang Dong [a], Chuanmao Zhang [b], Xianyu Lu [a], Jun Zhou [a,*]

[a] Department of Genetics and Cell Biology, College of Life Sciences, Nankai University, 94 Weijin Road, Tianjin 300071, China
[b] College of Life Sciences, Peking University, Beijing 100871, China

ARTICLE INFO

Article history:
Received 17 September 2007
Accepted 15 November 2007

Keywords:
Aurora kinases
Breast cancer
Spindle checkpoint
Mitosis
Apoptosis

ABSTRACT

Aurora kinases are key regulators of mitotic progression and have also been implicated in tumorigenesis. Small molecules that inhibit Aurora kinases have shown impressive anticancer activity in preclinical studies and are currently under clinical evaluation. In this study, our data show that suppression of Aurora activity with a specific inhibitor prevents the proliferation of breast cancer cells. Molecular modeling studies indicate that the Aurora inhibitor suppresses Aurora activity by competitive displacement of ATP. Mechanistically, the Aurora inhibitor causes the accumulation of multinucleated cells, leading to profound apoptosis in the absence of caspase-3 activity. Further studies show that the sensitivity of cancer cells to the Aurora inhibitor is independent of the spindle checkpoint. In addition, the Aurora inhibitor acts synergistically with the vinca alkaloids but not with the taxanes in inhibiting cell proliferation and inducing apoptosis. These results suggest that Aurora inhibitors might be effective in spindle checkpoint-defective cancer cells and a combination of Aurora inhibitors with the vinca alkaloids is a promising approach for cancer chemotherapy.

1. Introduction

The Aurora family of serine/threonine protein kinases plays a critical role in cell division [1,2]. In mammals, this family of kinases has three members, namely Aurora-A, -B, and -C, which differ in cellular localization and function. Aurora-A accumulates at centrosomes from S phase to the end of mitosis, and has been implicated in centrosome maturation and bipolar spindle assembly [3]. Aurora-B localizes at different places in the mitotic apparatus, depending on the stage of mitosis, and binds inner centromere protein, survivin, and borealin to form the chromosome passenger complex, which is important for chromosome attachment and segregation, and cytokinesis [1,4]. Aurora-C is localized at the centrosome during late mitosis and is functionally related to Aurora-B [1].

As essential mitotic regulators, Aurora kinases are required for the maintenance of genetic stability. Deregulation of Aurora expression or function might provoke genetic instability and lead to cancer. In fact, overexpression of these kinases has been detected in various human cancers [2,5–7], and Aurora-A has been identified as a cancer susceptibility gene [8].

The implication of Aurora kinases in tumorigenesis suggests that these kinases may serve as effective targets for the development of anticancer agents. A number of chemical compounds against Aurora kinases, notably ZM447439, Hesperadin, and VX-680, have been developed in the past years, and some of them have shown impressive anticancer activity in preclinical studies [7]. For example, VX-680 has been demonstrated to suppress tumor growth in rodent xenograft models [9], and the anticancer activity of this agent is currently being investigated in clinical trials. Because

* *Corresponding author*: Tel.: +86 22 2350 4946; fax: +86 22 2350 4946.
E-mail address: junzhou@nankai.edu.cn (J. Zhou).
0006-2952/$ – see front matter
doi:10.1016/j.bcp.2007.11.007

Aurora kinases are likely to act only in mitotic cells [10], their inhibitors might have better specificity in cancer treatment than the well known chemotherapeutic agents, such as microtubule-interfering agents and alkylating agents.

A key question regarding the mechanism of action of Aurora inhibitors is whether their efficacy against cancer cell proliferation depends on the integrity of the spindle checkpoint, a cellular surveillance mechanism that ensures accurate chromosome segregation during mitosis [11,12]. Given that defects in the spindle checkpoint are frequently observed in human cancers [13], elucidation of the checkpoint impact on the efficacy of Aurora inhibitors could provide important insights into the effective development of these agents in the clinic. This study was undertaken to explore the relationship between Aurora inhibitor activity and the spindle checkpoint status, and to further our understanding of the mechanisms of action of this group of agents.

2. Materials and methods

2.1. Materials

4-(4′-Benzamidoanilino)-6,7-dimethoxyquinazoline (BADIM) was purchased from Calbiochem. Paclitaxel, vinblastine, sulforhodamine B (SRB), 4′-6-diamidino-2-phenylindole (DAPI), propidium iodide (PI), and the mouse monoclonal antibody against α-tubulin were obtained from Sigma–Aldrich, and rhodamine-conjugated anti-mouse secondary antibody was from Jackson ImmunoResearch Laboratories.

2.2. Cells and adenoviruses

Human breast cancer cell line MCF7 was cultured in RPMI 1640 medium supplemented with 2 mM L-glutamine and 10% fetal bovine serum at 37 °C in a humidified atmosphere with 5% CO_2. Adenoviruses encoding dominant-negative Mad2 and BubR1 were prepared and amplified in low passage human embryonic kidney 293 cells as described previously [14]. Adenovirus titers were determined with an adenovirus titer kit (BD Biosciences).

2.3. Small interfering RNAs (siRNAs)

Mad2, BubR1, and luciferase siRNAs were designed to target Mad2 sequence 5′-ACCTTTACTCGAGTGCAGA-3′, BubR1 sequence 5′-CAATACTCTTCAGCAGCAG-3′, and luciferase sequence 5′-CGTACGCGGAATACTTCGA-3′, respectively. The siRNAs were synthesized by Dharmacon and transfected to cells with the lipofectamine 2000 reagent following the manufacturer's instruction (Invitrogen).

2.4. Molecular modeling

BADIM was docked onto the 1.9-Å coordinates obtained from the crystal structure of Aurora-A [15], using standard DOCK methodology [16]. The lowest-energy Aurora-A/BADIM interaction model is shown in Fig. 1.

2.5. In vitro cell proliferation assay

Cells grown in 96-well plates were treated with gradient concentrations of BADIM for 48 h. SRB-based cell proliferation assays were then performed as described previously [17]. The percentage of cell proliferation as a function of drug concentration was plotted to determine the IC_{50} value, which stands for the drug concentration needed to prevent cell proliferation by 50%.

2.6. Flow cytometry

Flow cytometric evaluation of cellular DNA content was performed as described [14]. Briefly, 2×10^6 cells were collected, washed twice with ice-cold phosphate-buffered saline (PBS), and fixed in 70% ethanol for 24 h. Cells were washed again with PBS and incubated with PI (20 μg/ml)/RNaseA (20 μg/ml) in PBS for 30 min in the dark. Samples were analyzed on a BD FACSCalibur flow cytometer.

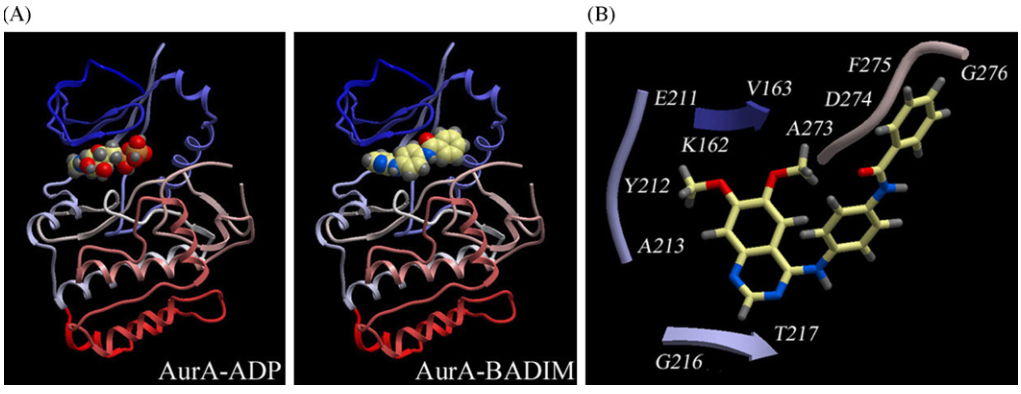

Fig. 1 – Molecular modeling of the interaction between BADIM and Aurora-A. (A) Schematic models showing Aurora-A with ADP (left panel) or BADIM (right panel). The Aurora-A/ADP model was derived from the coordinates for the crystal structure of the Aurora-A/ADP complex [15], and the Aurora-A/BADIM model was created by molecular docking as described in Section 2. (B) Details of important interactions between BADIM and Aurora-A. BADIM is color coded with red depicting oxygen, blue depicting nitrogen, yellow showing carbon, and grey representing hydrogen. Amino acid residues of Aurora-A involved in the interaction with BADIM are labeled.

2.7. Immunofluorescence microscopy

Cells grown on glass coverslips were fixed with cold (−20 °C) methanol for 5 min and then washed with PBS for 5 min. Nonspecific sites were blocked by incubating with 2% bovine serum albumin in PBS for 15 min. Cells were incubated with mouse monoclonal anti-α-tubulin antibody for 2 h and then rhodamine-conjugated anti-mouse secondary antibody for 1 h followed by staining with DAPI for 5 min. Coverslips were mounted with 90% glycerol in PBS and examined with an Olympus fluorescence microscope.

2.8. Apoptosis assays

Annexin V staining of the apoptotic membranes was performed by using the annexin V apoptosis detection kit (FITC) following the manufacturer's protocol (Pharmingen). DNA strand breaks were identified using the terminal deoxynucleotidyltransferase-mediated dUTP nick-end labeling (TUNEL) assay kit (molecular probes). Caspase-3 activity was measured by the cleavage of the small synthetic substrate Z-DEVD-aminoluciferin (Promega) that becomes luminogenic upon cleavage. The luminescent signal is directly proportional to the amount of caspase-3 activity.

2.9. Analysis of combined drug effects

Cells were treated with a range of BADIM and paclitaxel (or vinblastine) concentrations alone and in combination at a fixed ratio of 1000:1 for 48 h. At the end of this period, the inhibition of cell proliferation was measured for each condition. Treatment interaction effects of BADIM and paclitaxel (or vinblastine) were then determined by calculating the combination index (CI) values for each fraction affected using the commercially available CalcuSyn program (Biosoft), which is based on the median-effect principle of Chou and Talalay [18]. The CalcuSyn program automatically analyzes a data set using both the mutually exclusive assumption (similar mechanisms of action of both drugs) and the mutually nonexclusive assumption (dissimilar mechanisms of action of both drugs). The CI equation determines the additive effect of drug combinations, such that synergism is defined as a greater-than-the-expected-additive effect, and antagonism is defined as less-than-the-expected-additive effect. Thus, CI values less than 1 correspond to synergistic drug interactions, CI values equal to 1 correspond to additive interactions, and CI values greater than 1 correspond to antagonistic interactions.

3. Results

3.1. Molecular modeling of the interaction between BADIM and Aurora-A

BADIM is a cell-permeable anilinoquinazoline compound that potently and selectively inhibits the activity of both Aurora-A and Aurora-B [19]. To gain mechanistic insight into how BADIM exerts such an inhibitory effect, we simulated the interaction of BADIM with Aurora-A by molecular modeling. BADIM was docked onto the 1.9-Å coordinates obtained from the crystal structure of Aurora-A [15], and the lowest-energy interaction model was then generated. As shown in Fig. 1A, a bi-lobal shape characteristic of protein kinases was presented by the model, and the BADIM binding pocket was situated between the two lobes, where the ATP/ADP binding pocket resides [15]. A detailed examination of the molecular interaction revealed amino acid residues on Aurora-A that are involved in BADIM binding, including K162–V163, E211 ~ A213, G216–T217, and A273–G276 (Fig. 1B), many of which are critical for ATP/ADP interaction with Aurora-A [15]. These data indicate that BADIM is likely to inhibit Aurora activity by competitive displacement of ATP, like the action of many other Aurora inhibitors.

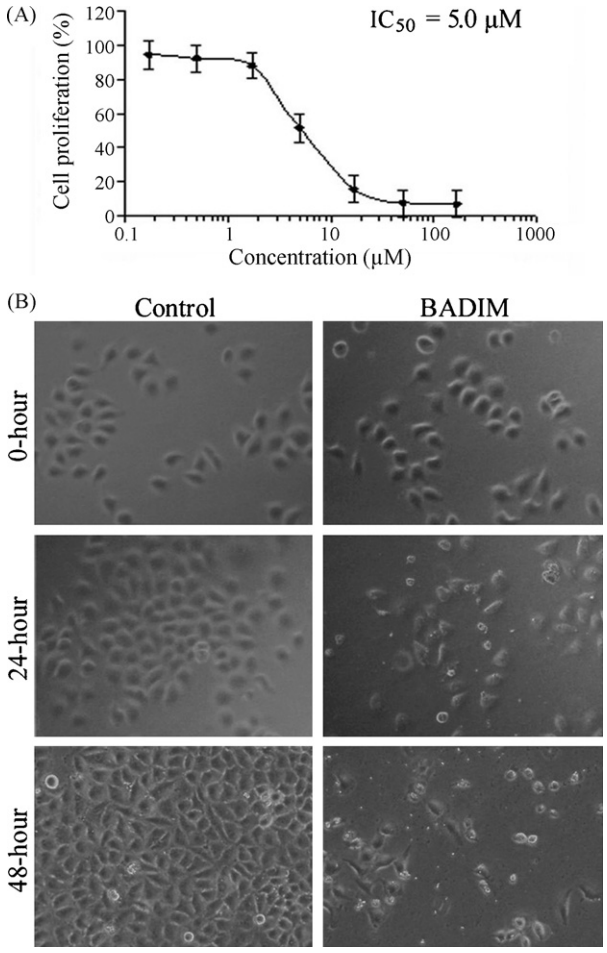

Fig. 2 – Inhibition of Aurora activity with BADIM prevents the proliferation of human breast cancer cells. (A) MCF7 cells were treated with varying concentrations of BADIM for 48 h, and the percentage of cell proliferation was measured by SRB-based in vitro cell proliferation assay. The drug concentration needed for 50% inhibition of cell proliferation (IC_{50}) is shown at the upper side. Values, means of three independent experiments; bars, SD. (B) Phase contrast images of MCF7 cells treated with 5 μM BADIM or equal volume of the DMSO control for 0, 24, or 48 h.

3.2. *Inhibition of Aurora activity with BADIM prevents the proliferation of human breast cancer cells*

Suppression of Aurora kinase activity by compounds such as ZM447439, Hesperadin, and VX-680 has been demonstrated to inhibit cancer cell proliferation [7]. In this study, we examined whether the Aurora inhibitor BADIM has a similar anti-proliferative activity. MCF7 human breast cancer cells were treated with gradient concentrations of BADIM, and its effect on cell proliferation was then evaluated by SRB staining assay. We found that BADIM prevented the proliferation of MCF7 cells in a concentration-dependent manner, and the IC_{50} value, which stands for the drug concentration needed to prevent cell proliferation by 50%, was determined to be 5.0 μM (Fig. 2A). Phase contrast microscopic analysis of the cell morphology revealed that while MCF7 cells proliferated normally in DMSO-treated cells, their proliferation was significantly impaired in the presence of BADIM (Fig. 2B). Together these results demonstrate a potent anti-proliferative activity for the Aurora inhibitor BADIM.

3.3. *BADIM causes the accumulation of multinucleated cells, leading to apoptotic cell death*

To better understand the mechanism of action of BADIM, we examined the morphology of microtubules and DNA of BADIM-treated cells by immunofluorescence microscopy. We found that this agent caused the accumulation of cells with multi-lobed nuclei (Fig. 3A), suggesting a failure of cytokinesis. For example, 16% of BADIM-treated cells had multi-lobed nuclei upon treatment with 5 μM BADIM for 24 h, whereas multinucleated cells were rarely detected in the control group (Fig. 3B).

Examination of MCF7 cells treated with BADIM for a longer period revealed that this agent induced the formation of condensed and fragmented nuclei characteristic of apoptosis (Fig. 4A). The induction of apoptosis by BADIM exhibited a time-dependent manner. For example, 7.3% and 39.8% of cells underwent apoptosis upon treatment with 5 μM BADIM for 24 and 48 h, respectively (Fig. 4B). We then performed flow cytometry to further examine BADIM-induced apoptosis. MCF7 cells treated with BADIM for 48 h were collected and stained with the DNA dye PI, and cellular DNA content was analyzed by a flow cytometer. The percentage of cells with less than 2N DNA content (sub-G1 cell population) was quantified as a measure of apoptosis. BADIM was found to increase the percentage of sub-G1 cells (Fig. 4C). In addition, consistent with the multinucleation induced by BADIM, a subset of cells was found to be polyploid upon BADIM treatment (Fig. 4C).

To investigate further whether BADIM-treated cells die through the apoptosis pathway, we performed annexin V staining assay, which reports the loss of phosphatidylserine asymmetry of plasma membrane at the early stage of apoptosis. As shown in Fig. 4D, BADIM induced the accumulation of annexin V-positive cells. We also performed TUNEL assay, which detects DNA breaks in the process of apoptosis, and found that BADIM increased TUNEL-positive cells (Fig. 4E). These results indicate that MCF7 cells are committed to die by apoptosis upon BADIM treatment.

We then measured caspase-3 activity in BADIM-treated cells, using the small synthetic substrate Z-DEVD-aminoluciferin. As shown in Fig. 4F, BADIM did not increase caspase-3 activity in MCF7 cells, although it significantly increased caspase-3 activity in CEM lymphoblastoid cells. This finding is consistent with the previous observations that MCF7 cells lack caspase-3 activity and can die in the absence of caspase-3 activity [20,21], and suggests that MCF7 cells die by non-canonical apoptosis upon BADIM treatment.

3.4. *BADIM-induced apoptosis is independent of the spindle checkpoint*

To test whether BADIM is effective in cancer cells that harbor spindle checkpoint defects, we knocked down the expression of two essential components of the spindle checkpoint, Mad2 and BubR1 [11], to inhibit the spindle checkpoint function. MCF7 cells were transfected with Mad2, BubR1, or control siRNAs for 24 h and then treated with 5 μM BADIM or 50 nM paclitaxel for 0, 12, 24, or 36 h. The percentage of mitotic cells was quantified by immunofluorescence microscopy. As

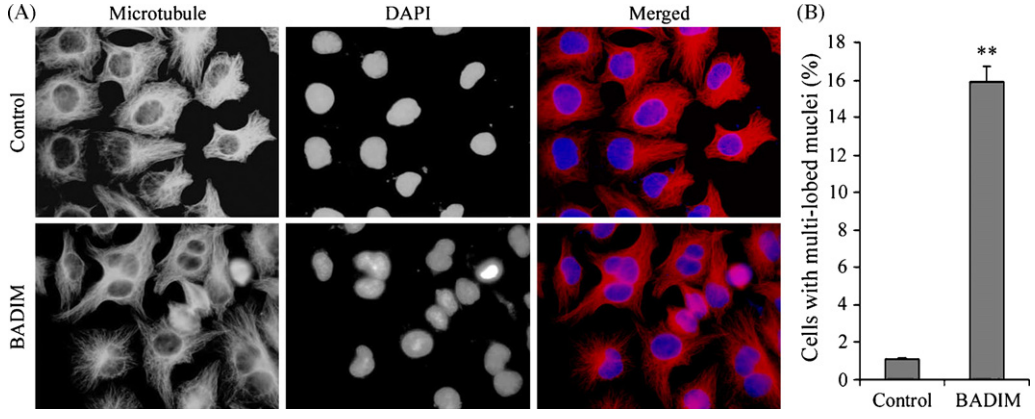

Fig. 3 – BADIM results in the accumulation of multinucleated cells. (A) Immunofluorescence images of microtubules (red) and DNA (blue) in cells treated for 24 h with 5 μM BADIM or DMSO (control). (B) Experiments were performed as in (A), and the percentage of multinucleated cells was then quantified. Values, means of three independent experiments; bars, SD; **, $P < 0.01$.

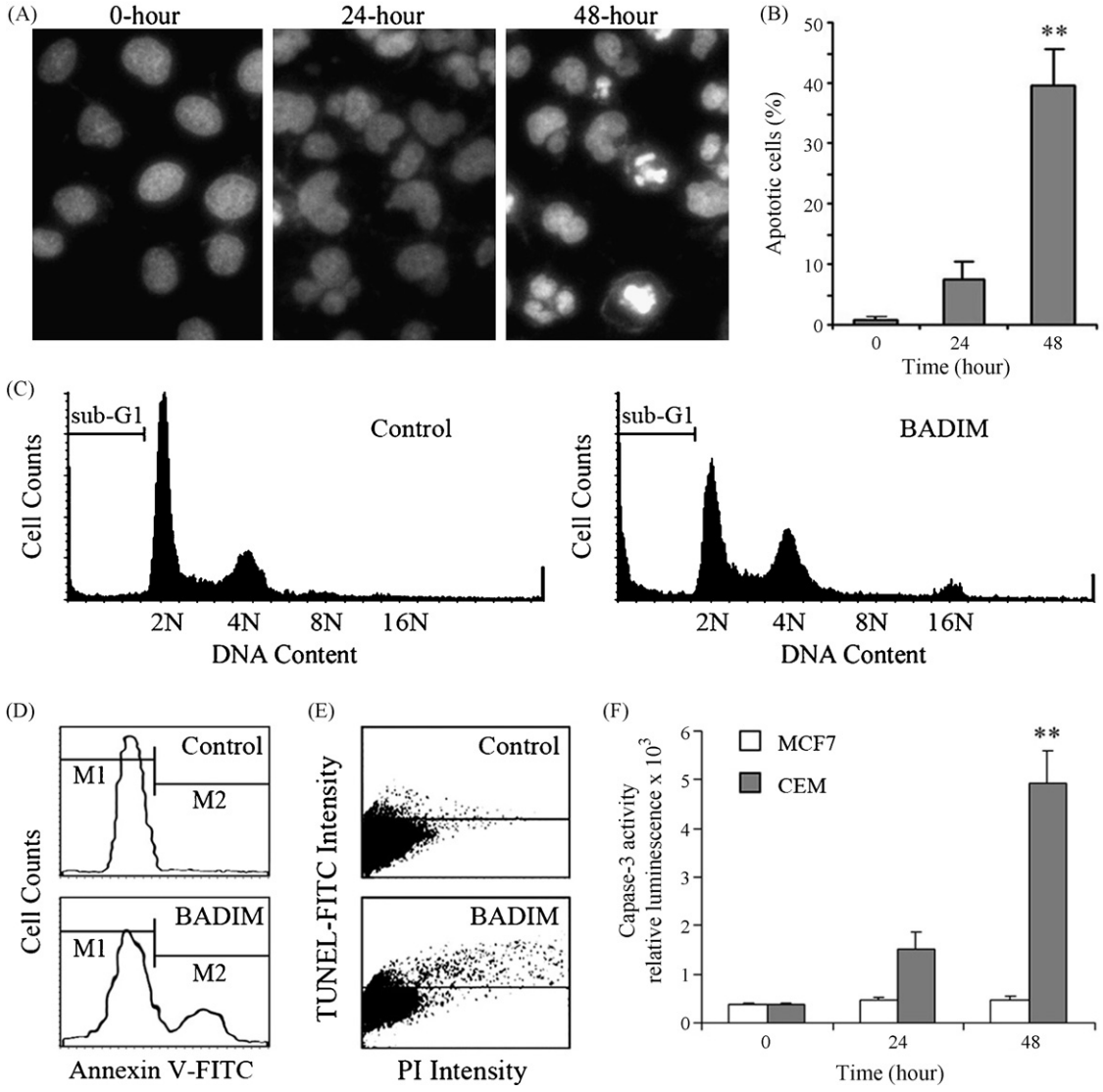

Fig. 4 – BADIM triggers apoptosis in breast cancer cells. (A) MCF7 cells were treated for 0, 24, or 48 h with 5 μM BADIM and stained with the DNA dye DAPI. The nuclear morphology of cells was then observed under a fluorescence microscope. Apoptotic cells exhibit condensed and fragmented nuclei. (B) Experiments were performed as in (A), and the percentage of cells with apoptotic nuclear morphology was quantified. (C) Flow cytometric analysis of DNA content in MCF7 cells treated for 48 h with 5 μM BADIM or DMSO (control). BADIM treatment resulted in a clear increase in the percentage of cells with less than 2N DNA content (sub-G1 population). (D) Quantitation of apoptosis by annexin V staining in MCF7 cells treated for 48 h with 5 μM BADIM or DMSO (control). The M1 and M2 gates indicate annexin V-negative and -positive staining populations, respectively. (E) Quantitation of apoptosis by TUNEL analysis in MCF7 cells treated for 48 h with 5 μM BADIM or DMSO (control). (F) Quantitation of caspase-3 activity in MCF7 and CEM cells treated with 5 μM BADIM for 0, 24, or 48 h. Caspase-3 activity was analyzed using the luminogenic substrate Z-DEVD-aminoluciferin. Values, means of three independent experiments; bars, SD; **, $P < 0.01$.

shown in Fig. 5A, siRNA-mediated knockdown of Mad2 or BubR1 remarkably inhibited the ability of paclitaxel to arrest cells at mitosis, indicating that the siRNAs could impair the spindle checkpoint. In contrast, no significant mitotic arrest was observed for BADIM treatment, either in control siRNA or Mad2/BubR1 siRNA-transfected cells. We then examined the effects of the siRNAs on paclitaxel- and BADIM-induced apoptosis in MCF7 cells. Cells were transfected with Mad2, BubR1, or control siRNAs for 24 h and then treated with 5 μM BADIM or 50 nM paclitaxel for 48 h. The percentage of apoptotic cells was quantified by fluorescence microscopic analysis of nuclear morphology. Consistent with previous findings [22,23], our data revealed that knockdown of Mad2 or BubR1 significantly prevented paclitaxel-induced apoptosis (Fig. 5B). In contrast, BADIM-induced apoptosis was not obviously affected by knockdown of Mad2 or BubR1 (Fig. 5B). Similar results were achieved by using adenoviruses expressing dominant negative Mad2 and BubR1. As shown in Fig. 5C

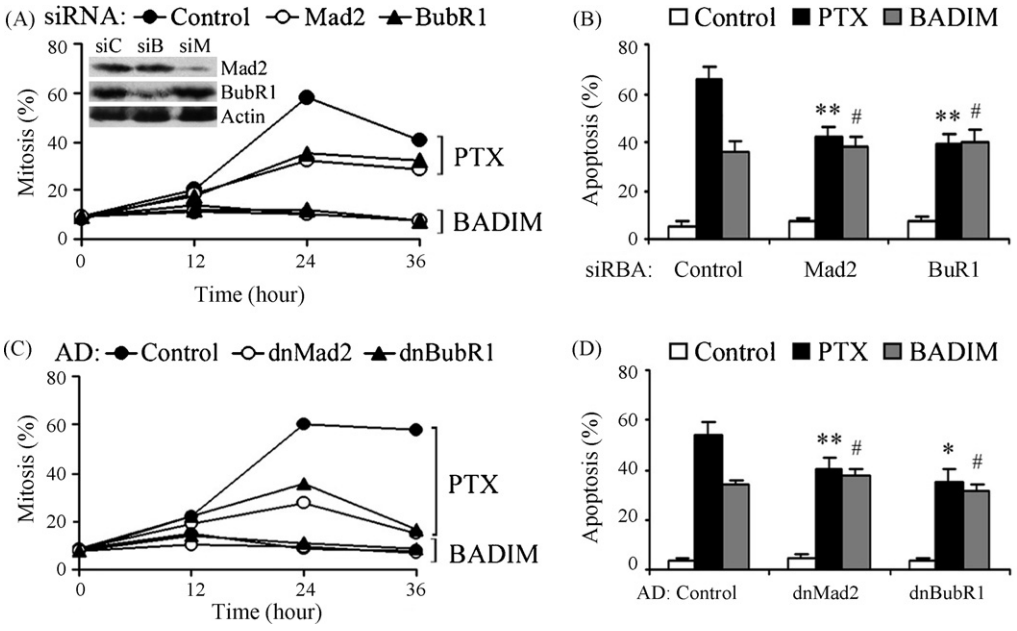

Fig. 5 – BADIM-induced apoptosis is independent of the spindle checkpoint. (A) Cells were transfected with Mad2, BubR1, or luciferase (control) siRNAs for 24 h and then treated with 5 μM BADIM or 50 nM paclitaxel (PTX) for 0, 12, 24, or 36 h. The percentage of mitotic cells was quantified by immunofluorescence microscopic analysis of microtubules and DNA. (Inset) Western blot analysis of the expression of Mad2, BubR1, and β-actin in cells transfected with Mad2, BubR1, or control siRNAs. siC, control siRNA; siB; BubR1 siRNA; siM, Mad2 siRNA. (B) Cells were transfected with Mad2, BubR1, or control siRNAs for 24 h and then treated with 5 μM BADIM or 50 nM paclitaxel for 48 h. The percentage of apoptotic cells was quantified by fluorescence microscopic analysis of nuclear morphology. (C) Cells were treated with dominant negative Mad2 (dnMad2), dominant negative BubR1 (dnBubR1), or β-galactosidase (control) adenoviruses for 24 h and then treated with 5 μM BADIM or 50 nM paclitaxel for 0, 12, 24, or 36 h. The percentage of mitotic cells was quantified as in (A). (D) Cells were treated with dnMad2, dnBubR1, or control adenoviruses for 24 h and then treated with 5 μM BADIM or 50 nM paclitaxel for 48 h. The percentage of apoptotic cells was quantified as in (B). Values, means of three independent experiments; bars, SD; #, $P > 0.1$; *, $P < 0.05$; **, $P < 0.01$.

and D, impairment of spindle checkpoint function by the dominant negative adenoviruses could inhibit the efficacy of paclitaxel to induce mitotic arrest and apoptosis. However, the adenoviruses did not significantly influence the sensitivity of MCF7 cells to the Aurora inhibitor BADIM. These results indicate that BADIM-induced apoptosis is independent of the spindle checkpoint.

3.5. *BADIM acts synergistically with the vinca alkaloids but not with the taxanes in inhibiting MCF7 cell proliferation and inducing apoptosis*

The mechanism of action of the Aurora inhibitor BADIM is clearly different from that of microtubule inhibitors, whose sensitivity depends on a functional spindle checkpoint. However, both BADIM and microtubule inhibitors inhibit cell proliferation and induce apoptosis. Thus, we wanted to investigate whether the combination of BADIM with microtubule inhibitors would result in a synergistic inhibition of cell proliferation and induction of apoptosis. We treated MCF7 cells with varying concentrations of BADIM and paclitaxel alone and in combination at a fixed ratio of 1000:1 for 48 h. At the end of this period, the inhibition of cell proliferation was measured by the SRB assay for each condition. Treatment interaction effects of BADIM and paclitaxel were then determined by calculating the CI values for each fraction affected using the CalcuSyn program, based on the principle of Chou and Talalay [18]. Such analysis yielded CI values greater than 1 for the combination of BADIM with paclitaxel, corresponding to an antagonistic interaction between these two drugs (Fig. 6A). In contrast, the CI values were less than 1 for the combination of BADIM with vinblastine, indicating a synergistic interaction between these two drugs (Fig. 6B). Nuclear morphology analysis further revealed that BADIM substantially potentiated vinblastine-induced apoptosis, but not paclitaxel-induced apoptosis (Fig. 6C and D). Similarly, BADIM was antagonistic with docetaxel, but synergistic with vincristine in inhibiting MCF7 cell proliferation and inducing apoptosis (data not shown).

4. Discussion

Chemotherapy represents one of the major treatment options to cancer patients. Unfortunately, side effects have significantly impeded the use of currently available drugs. Consequently, it is necessary to develop novel anticancer agents that have reduced side effects and better pharmacological profiles. Small mole-

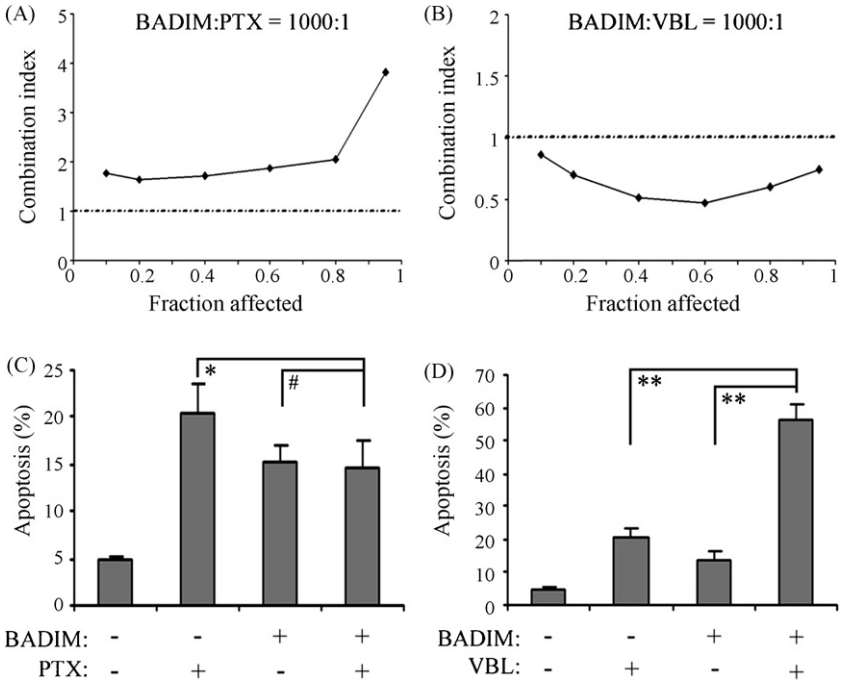

Fig. 6 – BADIM acts synergistically with vinblastine but not with paclitaxel in inhibiting MCF7 cell proliferation and inducing apoptosis. (A) Cells were treated with varying concentrations of BADIM and paclitaxel (PTX) alone and in combination at a fixed ratio of 1000:1 for 48 h. At the end of this period, the inhibition of cell proliferation was measured by the SRB assay for each condition. Treatment interaction effects of BADIM and paclitaxel were then determined by calculating the CI values for each fraction affected using the CalcuSyn program. CI < 1, synergistic drug interaction; CI = 1, additive drug interaction; CI > 1, antagonistic drug interaction. (B) Experiments were performed as in (A) except that vinblastine (VBL) was used instead of paclitaxel. (C) Percentage of apoptosis in cells treated for 48 h with 2 μM BADIM, 2 nM paclitaxel, or a combination of the two. (D) Percentage of apoptosis in cells treated for 48 h with 2 μM BADIM, 2 nM vinblastine, or a combination of the two. Values, means of three independent experiments; bars, SD; #, $P > 0.1$; *, $P < 0.05$; **, $P < 0.01$.

cules that inhibit Aurora kinases have emerged over the past years as a novel class of cancer chemotherapeutics. Because these kinases are only expressed and active as kinases in mitotic cells [10], their inhibitors might spare the non-proliferating cells and have higher specificity than current chemotherapeutics. In the present study, our data demonstrate that BADIM, a cell-permeable Aurora inhibitor, potently inhibits the proliferation of human breast cancer cells. This finding underscores the potential of Aurora kinases as valuable therapeutic targets for the treatment of breast cancer.

Mechanistically, our study has docked BADIM to the ATP/ADP pocket on Aurora-A, indicating that this agent might inhibit Aurora kinase activity through competitive binding with respect to ATP, like the action of many other Aurora inhibitors [7]. Biochemical studies are warranted, however, to investigate this possibility. The data presented in this study reveal that BADIM causes the accumulation of cells with multi-lobed nuclei, leading to apoptotic death. Given that Aurora kinases play an important role in cytokinesis [1,2], BADIM-induced multinucleation might be due to a failure of cytokinesis. The following apoptosis in turn might result from an alteration in the cytoplasm/nucleus ratio, which is known to be critical for cell viability. It is worth noting that multinucleation and subsequent apoptosis are also observed upon inhibition of several other kinases such as Polo-like kinases [24]. Therefore, it might be interesting to investigate in the future whether BADIM interacts with other apoptosis-inducing kinases in addition to Aurora kinases.

The spindle checkpoint acts as a molecular safeguard to ensure the fidelity in chromosome transmission during mitosis. It delays anaphase onset until all chromosomes are properly attached to the mitotic spindle [11,12]. Defects in the spindle checkpoint have been observed in many types of human cancers [13], and demonstrated to influence the efficacy of spindle-targeted drugs, including microtubule inhibitors and Eg5 inhibitors [25,26]. Interestingly, in this study, we find that the sensitivity of cancer cells to the Aurora inhibitor BADIM does not depend on a functional spindle checkpoint. The difference between BADIM and microtubule/Eg5 inhibitors in spindle checkpoint requirement is consistent with robust mitotic arrest following microtubule/Eg5 inhibitor treatment yet rather weak mitotic arrest when cells are exposed to the Aurora inhibitor. On the other hand, the difference might reflect fundamentally distinct mechanisms of action of these two groups of agents. Given that Aurora kinases per se are involved in the spindle checkpoint machinery, inhibition of Aurora activity by BADIM would compromise the checkpoint function; in this scenario, it is not difficult to understand why Mad2 or BubR1 siRNAs do not obviously decrease Aurora inhibitor sensitivity.

Synergistic drug combination is an important strategy in chemotherapeutic management of human cancer, which has

apparent advantages over the use of a single agent, such as reducing drug resistance and side effects and increasing drug efficacy [27]. Microtubule inhibitors, mainly referring to the taxanes and vinca alkaloids, have proven useful in the treatment of certain types of cancers [28]. However, their effectiveness in the clinic is significantly impaired by various side effects, notably neurological and hematological toxicities. Drug resistance is another notorious factor that thwarts the effectiveness of these agents [28,29]. Therefore, there has been a worldwide effort in the development of therapies using microtubule inhibitors combined with other chemical agents [27]. In this study, we find that the Aurora inhibitor BADIM acts synergistically with the vinca alkaloids but not with the taxanes in inhibiting cancer cell proliferation and inducing apoptosis. These findings suggest that a combination of Aurora inhibitors with the vinca alkaloids is a promising approach for cancer chemotherapy. In vivo studies are warranted to examine whether the vinca alkaloids synergize with Aurora inhibitors in inhibiting tumor growth. At represent, it remains elusive how the taxanes and vinca alkaloids have different BADIM-combination activities. One possibility is that the taxanes and vinca alkaloids may have different additional targets besides their common target—the microtubule, and inhibition of their additional targets may underlie their different BADIM-combination activities.

Acknowledgements

This work was supported in part by grants from the National Basic Research Program of China (2007CB914301), the Tianjin Natural Science Foundation (07JCZDJC03000), the Ph.D. Program Foundation (20060055008), and the New Century Excellent Talents Program (NCET-06-0217), Ministry of Education, China.

REFERENCES

[1] Carmena M, Earnshaw WC. The cellular geography of aurora kinases. Nat Rev Mol Cell Biol 2003;4:842–54.
[2] Fu J, Bian M, Jiang Q, Zhang C. Roles of Aurora kinases in mitosis and tumorigenesis. Mol Cancer Res 2007;5:1–10.
[3] Marumoto T, Zhang D, Saya H. Aurora-A—a guardian of poles. Nat Rev Cancer 2005;5:42–50.
[4] Adams RR, Carmena M, Earnshaw WC. Chromosomal passengers and the (Aurora) ABCs of mitosis. Trends Cell Biol 2001;11:49–54.
[5] Giet R, Petretti C, Prigent C. Aurora kinases, aneuploidy and cancer, a coincidence or a real link? Trends Cell Biol 2005;15:241–50.
[6] Meraldi P, Honda R, Nigg EA. Aurora kinases link chromosome segregation and cell division to cancer susceptibility. Curr Opin Genet Dev 2004;14:29–36.
[7] Keen N, Taylor S. Aurora-kinase inhibitors as anticancer agents. Nat Rev Cancer 2004;4:927–36.
[8] Ewart-Toland A, Briassouli P, de Koning JP, Mao JH, Yuan J, Chan F, et al. Identification of Stk6/STK15 as a candidate low-penetrance tumor-susceptibility gene in mouse and human. Nat Genet 2003;34:403–12.
[9] Harrington EA, Bebbington D, Moore J, Rasmussen RK, Ajose-Adeogun AO, Nakayama T, et al. VX-680, a potent and selective small-molecule inhibitor of the Aurora kinases, suppresses tumor growth in vivo. Nat Med 2004;10:262–7.
[10] Walter AO, Seghezzi W, Korver W, Sheung J, Lees E. The mitotic serine/threonine kinase Aurora2/AIK is regulated by phosphorylation and degradation. Oncogene 2000;19:4906–16.
[11] Zhou J, Yao J, Joshi HC. Attachment and tension in the spindle assembly checkpoint. J Cell Sci 2002;115:3547–55.
[12] Musacchio A, Salmon ED. The spindle-assembly checkpoint in space and time. Nat Rev Mol Cell Biol 2007;8:379–93.
[13] Kops GJ, Weaver BA, Cleveland DW. On the road to cancer: aneuploidy and the mitotic checkpoint. Nat Rev Cancer 2005;5:773–85.
[14] Liu M, Aneja R, Liu C, Sun L, Gao J, Wang H, et al. Inhibition of the mitotic kinesin Eg5 up-regulates Hsp70 through the phosphatidylinositol 3-kinase/Akt pathway in multiple myeloma cells. J Biol Chem 2006;281:18090–7.
[15] Nowakowski J, Cronin CN, McRee DE, Knuth MW, Nelson CG, Pavletich NP, et al. Structures of the cancer-related Aurora-A, FAK, and EphA2 protein kinases from nanovolume crystallography. Structure 2002;10:1659–67.
[16] Kick EK, Roe DC, Skillman AG, Liu G, Ewing TJ, Sun Y, et al. Structure-based design and combinatorial chemistry yield low nanomolar inhibitors of cathepsin D. Chem Biol 1997;4:297–307.
[17] Zhou J, Liu M, Aneja R, Chandra R, Lage H, Joshi HC. Reversal of P-glycoprotein-mediated multidrug resistance in cancer cells by the c-Jun NH2-terminal kinase. Cancer Res 2006;66:445–52.
[18] Chou TC, Talalay P. Generalized equations for the analysis of inhibitions of Michaelis-Menten and higher-order kinetic systems with two or more mutually exclusive and nonexclusive inhibitors. Eur J Biochem 1981;115:207–16.
[19] Heron NM, Anderson M, Blowers DP, Breed J, Eden JM, Green S, et al. SAR and inhibitor complex structure determination of a novel class of potent and specific Aurora kinase inhibitors. Bioorg Med Chem Lett 2006;16:1320–3.
[20] Fornari Jr FA, Jarvis DW, Grant S, Orr MS, Randolph JK, White FK, et al. Growth arrest and non-apoptotic cell death associated with the suppression of c-myc expression in MCF-7 breast tumor cells following acute exposure to doxorubicin. Biochem Pharmacol 1996;51:931–40.
[21] Mansilla S, Priebe W, Portugal J. Mitotic catastrophe results in cell death by caspase-dependent and caspase-independent mechanisms. Cell Cycle 2006;5:53–60.
[22] Kasai T, Iwanaga Y, Iha H, Jeang KT. Prevalent loss of mitotic spindle checkpoint in adult T-cell leukemia confers resistance to microtubule inhibitors. J Biol Chem 2002;277:5187–93.
[23] Sudo T, Nitta M, Saya H, Ueno NT. Dependence of paclitaxel sensitivity on a functional spindle assembly checkpoint. Cancer Res 2004;64:2502–8.
[24] Strebhardt K, Ullrich A. Targeting polo-like kinase 1 for cancer therapy. Nat Rev Cancer 2006;6:321–30.
[25] Weaver BA, Cleveland DW. Decoding the links between mitosis, cancer, and chemotherapy: the mitotic checkpoint, adaptation, and cell death. Cancer Cell 2005;8:7–12.
[26] Yamada HY, Gorbsky GJ. Spindle checkpoint function and cellular sensitivity to antimitotic drugs. Mol Cancer Ther 2006;5:2963–9.
[27] Wilson L, Jordan MA. New microtubule/tubulin-targeted anticancer drugs and novel chemotherapeutic strategies. J Chemother 2004;16(Suppl. 4):83–5.
[28] Jordan MA, Wilson L. Microtubules as a target for anticancer drugs. Nat Rev Cancer 2004;4:253–65.
[29] Zhou J, Giannakakou P. Targeting microtubules for cancer chemotherapy. Curr Med Chem Anticancer Agents 2005;5:65–71.